

Relation of Mechanical Properties to Solid Rocket Motor Failure

KENNETH W. BILLS JR.* AND JAMES H. WIEGAND†
Aerojet-General Corporation, Sacramento, Calif.

Experimental studies of propellant specimen and motor behavior during failure provide insight into the probable mechanisms of failure in a composite propellant system. At low rates and high temperatures, failure results from at least two successive processes: first, a dewetting or breaking of the binder to oxidizer bonds, and second, a tearing in the binder structure initiated at points of stress concentration such as regions of binder-oxidizer dewetting. Stress-strain analysis of a motor shows the potential failure points, and a failure analysis indicates the required mechanical properties to withstand failure. Laboratory testing has given a method of classifying propellant behavior, an estimate of material failure variability, and a method of correlating the uniaxial with biaxial tensile properties and with rate and temperature of test. Uniaxial tensile properties are obtained more conveniently by laboratory measurements, but biaxial properties appear to be related more directly to inner bore grain cracking. Good correlations were demonstrated between motor failures in thermal cycling and the failure properties of the propellant from laboratory tests.

Introduction

SATISFACTORY operation of solid propellant motors under specified conditions of use requires that the mechanical properties of the propellant be adequate to maintain grain integrity. The qualitative evaluation tests formerly used are giving way to carefully defined measurements that provide data directly assessable against minimum or maximum limits established by stress and failure analysis. Such an analysis is performed preferably as part of the initial ballistic and motor design to insure that the design will not impose unusual and severe requirements that are difficult or impossible to meet with the mechanical properties of available solid propellant systems. Although certain vibrational environments and extended high-temperature storage offer problems beyond present stress analysis capability—in part because of the chemical and structural changes that can take place in the solid propellant—present state-of-the-art designs can be evaluated quantitatively. Recent progress in developing propellants with improved mechanical properties at both the low- and high-temperature extremes allows the meeting of many motor requirements through straightforward engineering analysis supported by correlations of laboratory measurements.

The design of an optimum motor begins with a morphological ballistic analysis of the several possible grain designs over a specified burning rate range and specific impulse level. The effect of the expected temperature limits for storage and firing on the selected designs is accomplished by performing a stress analysis on the configuration as affected by the proposed method of mounting the grain in the chamber.¹⁻³ Stress analysis, even with the computer, usually requires the assumption of simple regular shapes and the superposition of star point stresses. Complex configurations, particularly three-dimensional ones, can be treated experimentally on a scale model by frozen photoelastic analysis^{4,5} using a birefringent plastic that simulates the development of grain

stresses through shrinkage of the plastic on cure. After cure, the stress pattern is frozen into the model, which then is cut into slices for photoelastic examination. The stress analysis describes quantitatively the regions of maximum stress and strain in which failure may occur.

The maximum stress-strain values can be compared with the propellant properties determined under the same stress-strain environment and at rates of testing and temperatures comparable to those expected in the motor. Fortunately, all possible conditions of rate and temperature need not be tested in order to give values of sufficient accuracy, since empirical correlations are well established for many systems. New motor applications, however, often require combinations of properties for optimum performance which cannot be predicted accurately from available propellants, and experimental formulations of propellants must be prepared.

Once selection of the optimum design-propellant system has been made, reduction of the propellant system to a specific formulation is guided by target values of the properties measured in the same evaluation tests used to provide the initial design data. Careful attention is given during this phase to see that adequately severe conditions of temperature, humidity, and storage are imposed, such that the sensitivity of each promising formulation to these variables can be assessed rapidly.⁶ Extensive experience in the evaluation of propellants already in manufacture and field use is required to insure that inadequate properties are revealed and corrected before selection of the final candidate. Finally, evaluation of full scale manufacturing batches by a veritable battery of chemical and physical tests defines statistically the property values of the selected formulation and serves as a basis for setting realistic manufacturing specifications that will insure that production propellant will continue to meet all requirements.

Problems have occurred in the past on experimental and production motors which unexpectedly and seriously interfered with the course of development and production. In each case, the problems led to new research and development programs, which, in turn, led both to an understanding of the causes of the difficulties and to lines of development which produced propellants of significantly improved properties.

In this paper, the problems associated with failure analysis will be discussed, and methods of attack on the problem will be described. The methods of studying failure in the laboratory and of correlating the data will be considered first, followed by a discussion of modes of failure in solid propellant rocket motors and methods of handling each important mode.

Presented at the ARS Solid Propellant Rocket Conference, Philadelphia, Pa., January 30–February 1, 1963. The authors wish to acknowledge the advice and technical support of H. P. Briar, A. Messner, R. C. Sampson, and their associates. The support of the U. S. Air Force, Air Material Command, for an unclassified study program, the results of which provided a significant point of departure for the failure studies described here, is acknowledged gratefully.

* Department Manager, Mechanical Properties Department, Solid Rocket Plant.

† Manager, Ballistics and Mechanical Properties Senior Department 4520, Solid Rocket Plant. Member AIAA.

Failure in Solid-Composite Propellants

In rocket motor applications, two types of solid propellant grain failures are observed. First, the grain may deform beyond some allowable limit, or second, the material actually may fracture. The criterion for the former type of motor failure usually is a slump of the grain (without fracture) beyond a certain prescribed limit, whereas fracture is of primary concern when attempting to characterize the failure behavior of the material.

The most beneficial type of fracture study is to test a given material over a wide number of multiaxial stress fields and then to compare the observed failures with some of the well-known fracture theories. An excellent summary of these fracture theories and their graphic representation in three-dimensional stress-space and strain-space has been prepared by Blatz and his co-workers.⁷ These geometric representations are termed "failure surfaces" and indicate that materials whose properties fall within these surfaces are safe from fracture.

In the infinitesimal deformation regions, the shape of the failure surface based on a stress criterion is unchanged when plotted in either principal stress-space or principal strain-space except for the values of the parameters. The same effect would be true for a failure surface based on a strain criterion. However, in the finite deformation regions (which are pertinent to the case of propellant rupture), the representation is affected greatly by the choice of the parameters because of nonlinear stress-strain behavior. Hence, for a given surface in principal stress-space, there are a number of surfaces in principal strain-space.

There appears to be no universal failure criterion, and the success of any given hypothesis is dependent largely on the materials and testing conditions with which it is associated. For solid propellants, the experimental derivation of a suitable criterion is complicated greatly by the large failure strains and is complicated further by important time and temperature effects. Furthermore, a failure theory for solid propellants necessarily includes a study of failure probability with particular reference to those members of the population most likely to fail.

Phenomenological Studies of Propellant Failure

The failure process in solid propellant materials is complicated by a multiplicity of factors, of which "dewetting" (i.e., failure of the filler-binder bond) is perhaps the most important.⁷⁻⁹ This dewetting effect always precedes propellant rupture and may be considered to be the first step in the failure process. A phenomenological description of the dewetting behavior leads to a means of classifying propellants according to their dewetting behaviors.

In a broad sense, dewetting itself may be termed a "failure phenomenon" since it requires the creation of "critical" stresses initially to cause failure of an oxidizer-binder bond, after which the dewetting effect readily propagates to neighboring particles producing a band or region of these failures.^{9,10} This band normally lies perpendicular to the direction of straining and varies in thickness depending on a number of factors, including filler content, particle size distributions, the bond strength between the particle and the binder, and the binder strength properties. These dewetted regions are relatively weak and provide the sites for the future failure of the propellant specimen. Previous studies of the microscopic character of propellant rupture have shown it to follow two steps. First, upon application of strain, separations of the binder from the oxidizer take place, resulting in the formulation of elliptical vacuoles about the filler particles (see Fig. 1). Second, a tear is initiated in the binder at an apex of a vacuole and propagates perpendicularly to the direction of straining. A typical example of this dewetting character is shown in Fig. 2. The dewetting can be seen to

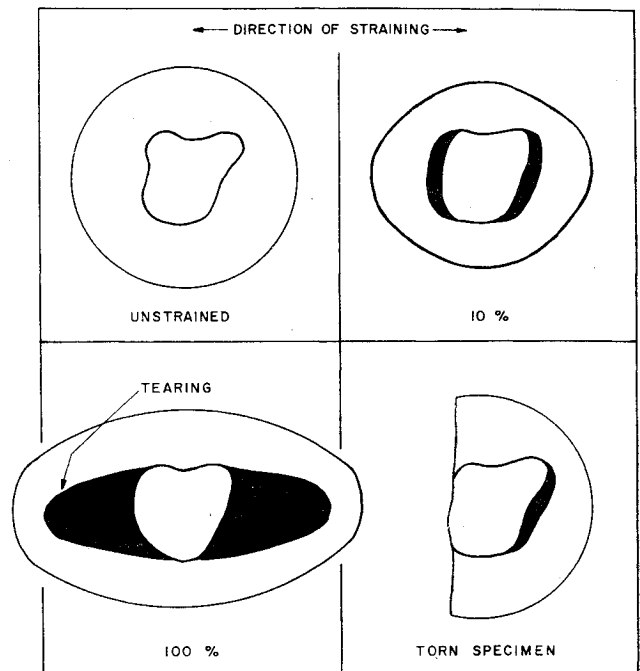


Fig. 1 Dewetting and tear around a particle embedded in a polymer.

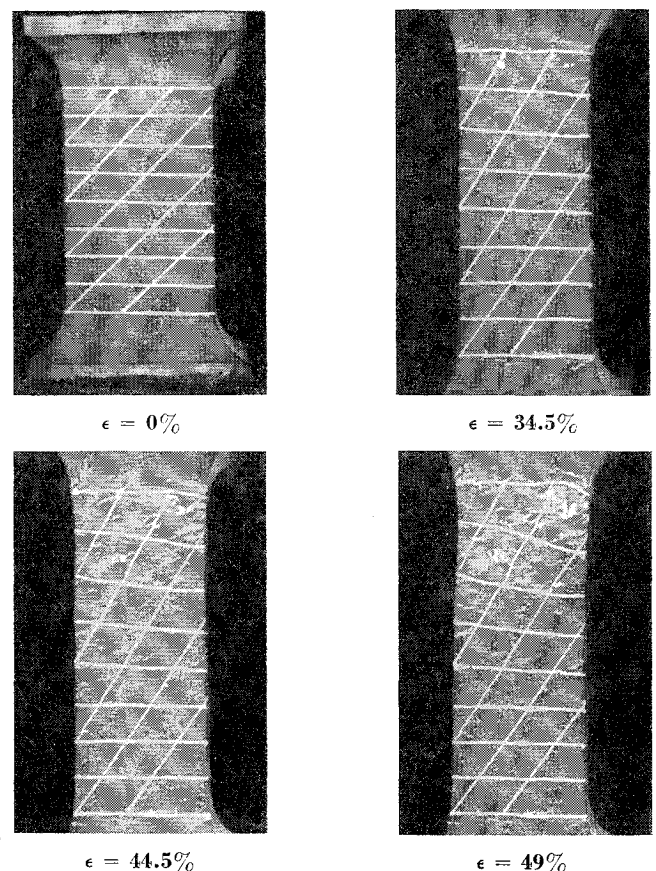


Fig. 2 Dewetting in propellant.

occur in localized regions, as evidenced by the whitish bands. The strain is not uniform throughout the test section. Such differences in local behavior profoundly affect methods of data analysis and predictions of behavior of propellants in rocket motors.

This dewetting phenomenon is observed also in biaxial loadings. However, in this case the localization effect produces bands in a honeycomb-type pattern as shown

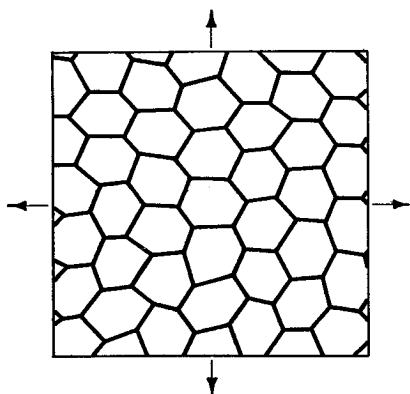


Fig. 3 Schematic representation of dewetting bands in a biaxially strained specimen.

schematically in Fig. 3. In this case, a number of oxidizer particles effectively agglomerate, permitting dewetting to occur around the periphery only. It is believed that this dewetting characteristic also will prevail in a triaxially loaded specimen, for which the dewetted agglomerates will be roughly spherical.

Recently developed composite propellants avoid this localization by chemical control of the binder-oxidizer interface to give uniform dewetting throughout the test section, as shown by the photomicrographs in Fig. 4.

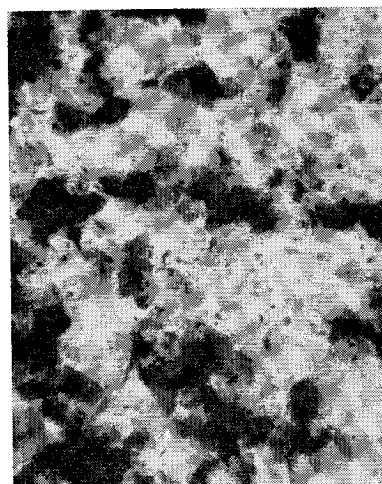
Propellant Classification for Failure

A classification system is proposed for propellant materials based upon their dewetting behavior. Four classes of propellants are proposed, as shown in Table 1.

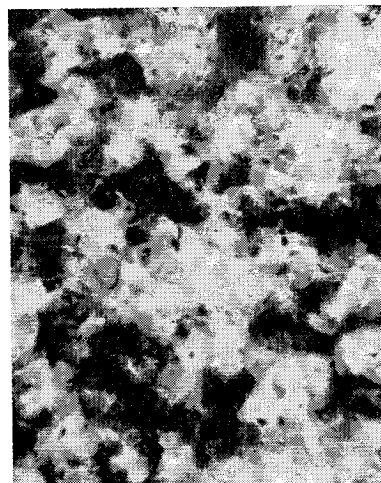
The dewetting character of a given composite propellant will change with temperature and strain rate. Thus, for example, a propellant may behave as a class 1 at temperatures above 100°F and as a class 4 at temperatures below -100°F. The dewetting character will shift gradually with decreasing temperature or increasing strain rate from the class 1 to the class 4 behavior. Most of the propellants

Table 1

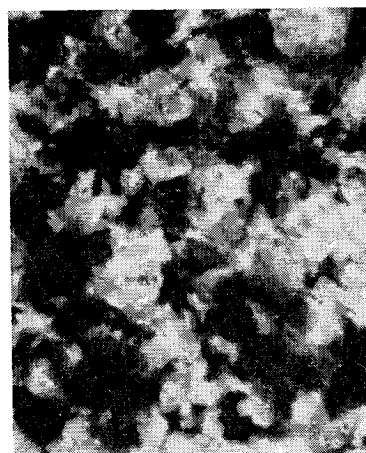
Class	Description	Mathematical relation
1	Essentially complete dewetting is observed as the break point is reached. (Figure 4 shows typical class 1 behavior.)	For the special case where dewetting may be considered complete at all points of strain, the finite deformation relations of Blatz ¹¹ offer a good first approximation. A mathematical description by strain energy functions appears to be the most promising approach.
2	Dewetting occurs in two or more bands throughout the gage length of the specimen. Local sites of dewetting occur generally throughout the specimen. (Figure 2 shows characteristic class 2 behavior.)	A mathematical approximation by strain energy functions appears to be the most promising approach.
3	Dewetting occurs generally in one narrow band only.	A mathematical approximation by strain energy functions appears to be the most promising approach.
4	No dewetting occurs up to the break point, typical of propellants below their glassy temperature.	The classical theory of elasticity applies quite well to these materials.



25% strain



50% strain



75% strain

Fig. 4 Dewetting in a class 1 solid propellant (44X, dark areas indicate the formation of cavities about the white oxidizer particles).

used today are class 1 or class 2 at 100°F and fall to class 3 (extending toward class 4) below 0°F. The effect of these changes in dewetting behavior is to shift the observed failure characteristics markedly with changes in temperature and strain rate. Generally, two characteristic failure types are observed. In the high-temperature and low-strain-rate regions (class 1 or class 2 behaviors), the failure tends to be of a ductile nature, whereas at the lower temperatures and higher strain rates (class 3 or class 4 behaviors), failure is a brittle fracture-type phenomenon.

Atmospheric moisture¹² acts upon the propellant differently at low (below 0°F) and at high temperatures (near 80°F). In the high-temperature region, the moisture ap-

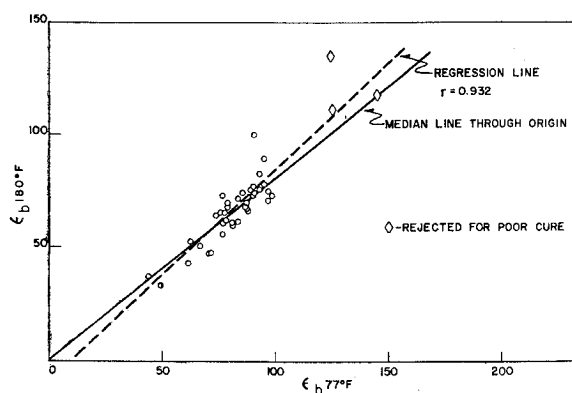


Fig. 5 Failure strain at 180°F vs that at 77°F.

parently promotes dewetting. At the lower temperatures, moisture tends to promote adhesion between the oxidizer and the binder, thus shifting the behavior toward that of a class 4 system. The effect upon the binder appears to be negligible. The overall result of this shifting toward a class 4 system is to increase the tensile strength and to decrease the failure strain.

The dewetting effect, and consequently the rupture behavior, is dependent primarily upon the adhesive bond between the binder and the oxidizer. The variability of this adhesive bond is believed to be the primary source of the variability encountered in mechanical properties measurements and failure testing. These comments are not intended to minimize specimen preparation and test design errors, but rather to point out the extreme importance of the effects of these adhesive bonds. It is well known in adhesion studies that trace quantities of certain impurities at the interface can modify adhesive bonds greatly. Such effects will predominate, even though great care is taken to standardize and monitor all other factors involved in the preparation of the bond. The magnitude of the effect of impurities is believed to be shown by the large testing variability between batches where coefficients of variation between 15 and 20% are typical for failure properties. This variability may be contrasted to within batch coefficients of variation of 3 to 5%. These latter variations are related primarily to testing and specimen preparation errors, whereas the former are dependent primarily upon material differences, among which the adhesive bond to the filler is believed to be the most variable.

Batch Variability of Failure Behavior

The large variability¹² associated with propellant properties suggests that certain batches and certain portions of these batches will be more susceptible to failure than others. A related hypothesis immediately is suggested for experi-

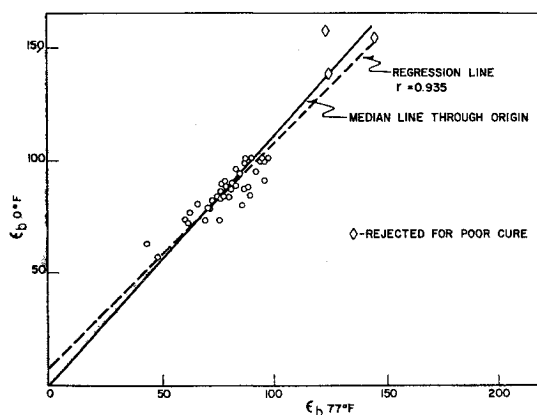


Fig. 6 Failure strain at 0°F vs that at 77°F.

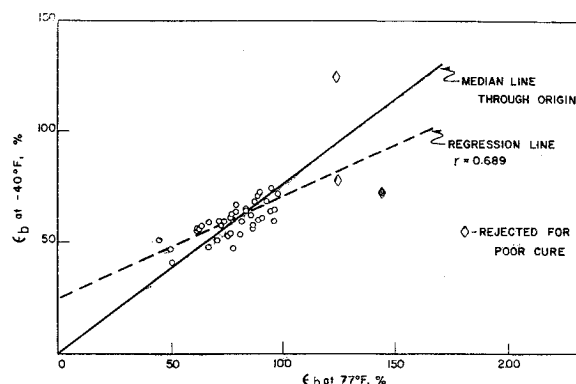


Fig. 7 Failure strain at -40°F vs that at 77°F.

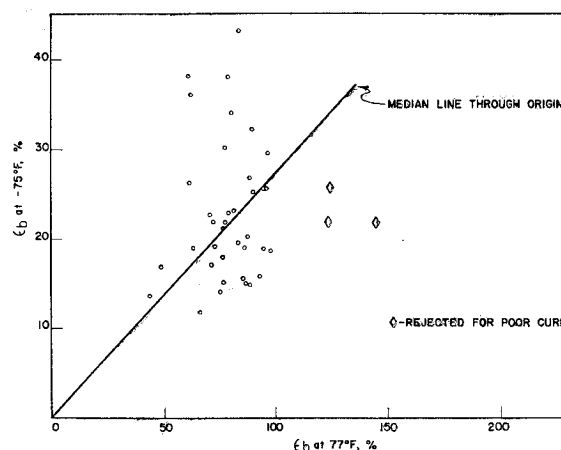


Fig. 8 Failure strain at -75°F vs that at 77°F.

mental testing: the failure behaviors under different types of stress-strain environments are related, such that those batches with the highest incidence of failure in one environment will have the highest incidence in another. It is clear that we lack the knowledge at this time to define failure mechanisms in detail for different batches or even different compositions.

The large-scale production of propellant at Aerojet-General Corporation offers the possibility of taking data on samples from different batches of propellant and determining the correlation between the failure values. A study of uniaxial data on one carton from each of 40 batches of a class 2 propellant was made on an Instron testing machine at the constant strain rate of 0.74 min^{-1} and at test temperatures from -75° to 180°F . The data are presented in the correlation graphs of the failure elongation at 77°F vs the same value at the other test temperatures for each of the cartons studied (see Figs. 5-8). The testing equipment used, the shape of the typical Joint Army-Navy-Air Force test specimen, and the type of force-time record obtained have been discussed previously by Wiegand.^{12, 6} The experimental data were analyzed numerically to give the correlation coefficients shown on each figure. These data gave high correlations from 0° to 180°F ; the three cartons giving highest elongations and the two giving lowest elongations were the same at all temperatures. These correlations would indicate that a test at any one of these test temperatures would have screened out the same extreme cartons of the population as a test at any other temperature. The data at -40° and at -75°F showed, however, that the correlation decreased steadily below 0°F . Since tests in the region of 0° to 180°F do not predict the relative order of quality among the batches at very low temperatures, our hypothesis of related failure behavior clearly is limited. This lack of correlation of quality outside of certain limits requires, therefore, a general study of each new system in order to

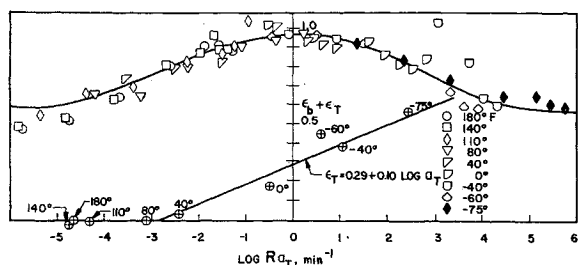


Fig. 9 Reduced failure strain of class 2 propellant obtained with vertical shift factor, ϵ_T , $t_s = -36^\circ\text{F}$.

define those limits within which relative quality is described statistically by any one test and outside of which additional tests are required. On the basis of such a study related to the environmental conditions of use, a minimum number of tests and test conditions can be selected to insure adequate quality in the finally accepted motors.

Constant Strain Rate Tensile Failure Correlation

The correlation of mechanical property behavior at different rates and temperatures has been performed on many polymers following the shift factor technique of Williams, Landel, and Ferry (WLF).¹³ The correlation of failure behavior for a rubber was shown by Smith and Stedry.^{14, 15} However, correlating the failure data in the highly filled polyurethane systems, such as the class 2 propellant, offers further problems. The maximum in the elongations-at-failure vs strain rate plot are not the same at different temperatures, this maximum decreasing as the temperature decreases. An extension of the WLF method analysis to these data has been performed by shifting the points, plotted as ϵ_b vs $\log R$ for each temperature, horizontally and also vertically as required to produce a continuous curve of ϵ_b vs $\log R a_T$. The vertical shift, not required for elastomers without filler, was done without regard to fitting a particular pattern. The results are shown in Fig. 9. These data proved more amenable to the correlation shown in Fig. 10, where the failure elongation is plotted vs temperature, the effect of rate of testing being shown by sliding the axes diagonally along a rate shift line. This type of graph has been the most useful when applied for the graphical comparison of propellant failure strains with the motor strains produced in thermal cycling.

Uniaxial vs Biaxial Tensile Failure Properties

To study the applicability of uniaxial tensile data to biaxial failure properties, especially as the latter apply at the inner bore of the grain, an experimental method is required to

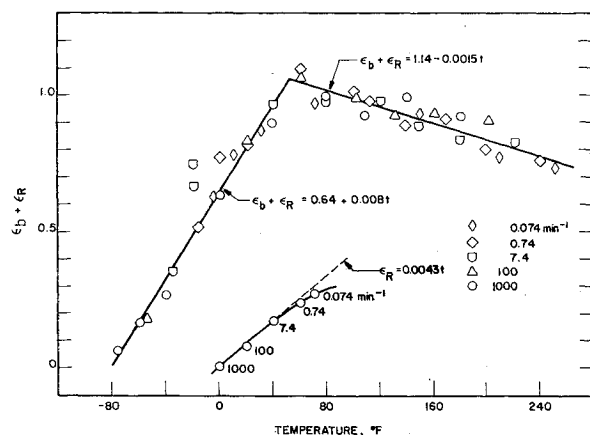


Fig. 10 Failure strain of a class 2 propellant with temperature using the diagonal shift technique.

Table 2 Relation between the failure strains in uniaxial and "strip biaxial" tension for typical class 2 propellants

Test temperature, °F	Strain rate, %/min.	Ratio of strains-at-break: uniaxial/biaxial		
		Propellant no. 1	Propellant no. 2	Propellant no. 3
110	10	1.0	1.1	1.3
	100	0.8	1.0	1.2
	1000	1.0	1.1	1.0
80	10	1.1	1.2	1.1
	100	1.2	1.2	1.0
	1000	1.0	...	1.1
40	10	1.0	1.1	1.2
	100	1.0	1.2	1.0
	1000	1.1	1.2	1.1
0	10	1.0	0.9	1.2
	100	0.9	1.5	1.1
	1000	1.1	1.1	1.1

simulate the biaxial strains met in the grain. The inner bore of a fully case-bonded grain under thermal cooling is restrained axially with relatively large hoop stresses and strains.^{3, 5} An experimental approximation to this condition employs the "strip biaxial" test specimen shown in Fig. 11. Within the testing region, the specimens are 0.25- × 7.0- × 1.0-in. gage length. The mode of testing is such as to restrain the specimen in one dimension while tensile straining it in a second and allowing it to deform as required in thickness. The lateral restraint is provided by bonding the specimen at the upper and lower edges to holders, which, to a fair extent, prevent lateral movement (contraction) of the specimen. As shown in Table 2, this test method provides failure strain data that are within $\pm 20\%$ of those obtained in uniaxial tensile tests. However, most of the uniaxial failure strains are between 0 and 20% greater than the biaxial failure strains. This relationship is expected in view of the stress field experienced by the biaxial specimen.

Thus, for any given propellant system, comparisons between the data from these two testing methods should make it possible to evaluate the relation between uniaxial failure strains and the inner bore hoop strains. Since the uniaxial specimens are prepared and tested most readily and more cheaply, this relation provides important economic interest.

Constant Strain Failure Data

The high modulus of rocket case materials relative to the low modulus of the propellant causes the strains developed at equilibrium temperatures to be determined chiefly by the difference in coefficients of thermal expansion of the case and

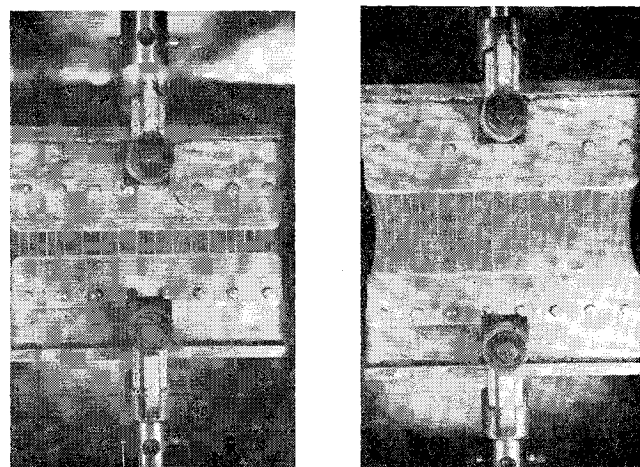


Fig. 11 Biaxial tension specimens unstrained and at $\lambda = 3.5$.

the propellant.^{1, 3} These differences force the propellant to adapt itself to high strains in the bore of thick-webbed motors and at the end discontinuities. The resulting failure behavior is that of a material failing under an essentially constant strain. Constant strain data show a characteristic failure incidence that increases regularly with the strain level and covers a wide range of failure times for a group of replicate specimens. Typical constant strain failure data are shown in Fig. 12, where the results are presented for 26 specimens of a class 2 propellant tested at 91% constant strain and 77°F. This large strain level was chosen to provide short failure time intervals. At lower strain levels the time to failure increases significantly, as shown in Fig. 13. To provide estimates of those strains that would not produce failure even after long test periods, the data are replotted, as shown in Fig. 14, so that extrapolation to $1/t = 0$ yields an estimate of a critical constant strain below which a minimum percentage of specimen failures would be expected. For this particular class 2 propellant, the critical constant strain (at a 90% survival level) would be estimated as 20%.

The selection of constant strain test conditions for a particular data analysis should be preceded by determination of survival curves. In the absence of such data, any statistical comparison of test data is based upon assumptions that may or may not be applicable. Where the number of specimens available is small, giving only one or two specimens at each strain level, only approximate estimates of quality can be obtained.

Correlation of Failure Data with Small Motor Failures

In the consideration of motor failures and their correlations with laboratory measurements on propellants, there are several aspects that must be remembered and considered. First, failure modes vary over the temperature range. Typically there are two types of failure, a low-temperature or "brittle-fracture" mode and a high-temperature or "ductile" (plastic) mode.¹² Second, the moisture content of the propellant greatly affects the failure strain levels at all temperatures. Third, the major part of the grain mass is subjected to small deformations. Hence, as a fair first approximation, the inner bore strains may be calculated using viscoelastic or elastic analysis. The elastic analysis is indicated when using long-term, near-equilibrium propellant properties. For the purposes indicated here, the long-term or elastic calculations were employed. Experiments on cycling small, tubular, case-bonded grains to low temperatures show good correlations between measured and calculated failure strains.

For star points and end discontinuities, the predictions of maximum strains from an elastic analysis with strain concentrations estimated from photoelastic experiments^{4, 5} also are reasonably good for low temperatures. They become increasingly poorer as the dewetting type of failure is approached at temperatures above 0°F. This trend is caused partly by the large deformations produced at high strains.

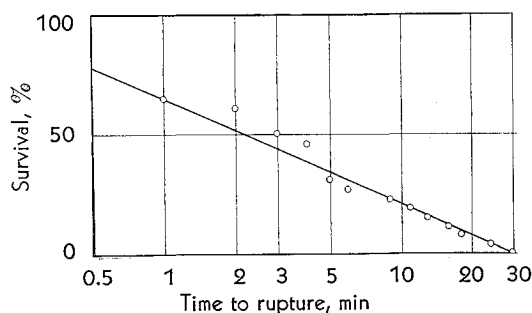


Fig. 12 Survival of specimens under constant strain (91%) vs time to rupture after straining.

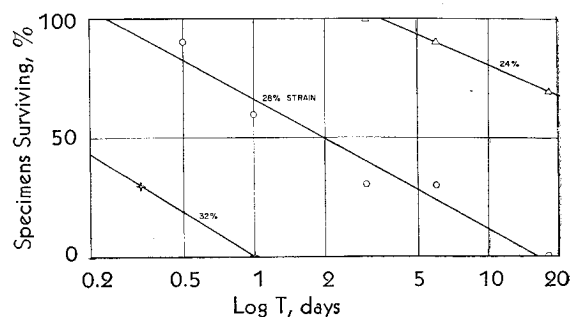


Fig. 13 Survival vs log time for three strain levels.

The deformations also reduce the accuracy of photoelastic analyses. These deformations have been studied in propellant grain segments when subjected to various large strains up to failure. In these tests, a comparison is made of the stresses in a grain model subjected to normal circumferential pressure loading with those stresses of a segment of a grain model loaded in tension along the edges of the segment. A 60° segment is cast of urethane rubber the same size and shape as one sector of symmetry of the star grain. A sheet of plate glass is cemented to each edge of the segment to form lips along the edges of the segment for applying load with two Lucite wedges cut to a 60° angle. The glass plates are wedged apart by placing one wedge on each side of the model to put the model in tension without bending or changing the angle of the segment. Figure 15 shows the star-point stress pattern in a portion of a full six-point star model under uniform external pressure compared with the stress pattern in the grain segment model. The method can be

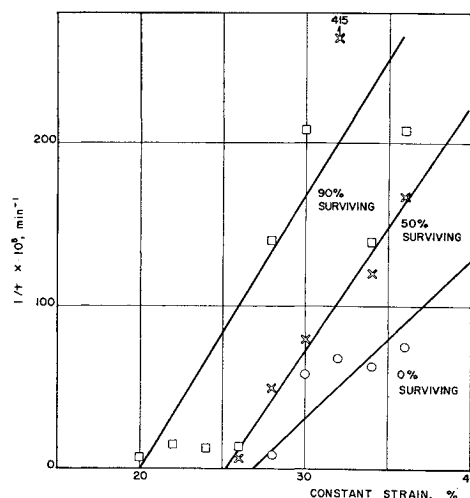


Fig. 14 Reciprocal failure time vs applied strain.

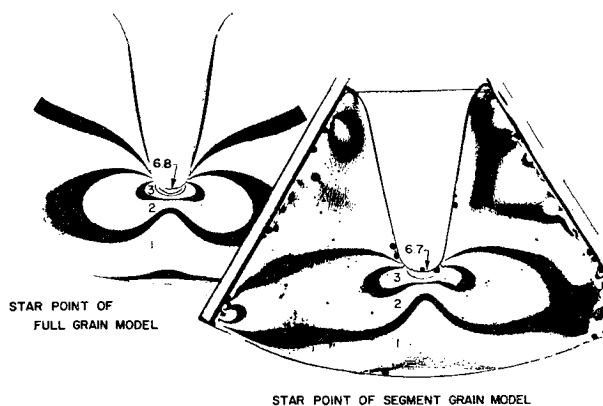


Fig. 15 Star point of full grain model and segment grain model.

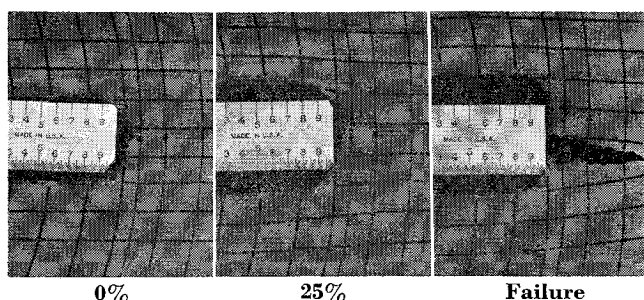


Fig. 16 Grid patterns on straining segment of live propellant.

seen to produce photoelastic stress patterns that are very nearly those of a full grain model subjected to uniform pressure. The application of the segment test to a live propellant segment can be seen in Fig. 16 to produce a distortion of the grid and finally failure. The grid pattern at 25% strain of the star point is superimposed on that at 0% in Fig. 17 to show the distortion more clearly.

A further difficulty in predicting strains near failure is the nonuniformity of the deformations produced by localized dewetting. In an overall sense, the correlation is reasonable because such localized dewetting also characterized specimen failure—the failure value of strain thus being an average strain value over the gage length—and because the correlation of failure data is not of a point or line type but rather of a statistical distribution of events from no-fail to all-fail. Such a distribution of failure behavior is observed in experimental work, as shown below for small motor cycling.

Low-Temperature Failure Mode

In one study,¹² small motors with case-in-case cylindrical grains of inner/outer diameter ratios from 4 to 12.5 were subjected to temperature cycling to -75°F . Grain failures were experienced in many cases. The propellants involved were of class 1 and class 2 types. At low temperatures, correlation for these failures was obtained by comparing the strain in the motor, as measured on the first cycle to -75°F , with the failure strain measured in the standard constant rate Instron test. The propellant failure strain used was the lowest tensile strain at break, $\epsilon_{b\min}$, reported from the two or three tensile tests taken at -75°F . The strain at break was divided by the maximum measured strain in the motor to give a ratio called $\epsilon_{b\min}/\epsilon_{mm}$, which is shown plotted against the percent of motors cracking at that ratio in Fig. 18. When the ratio $\epsilon_{b\min}/\epsilon_{mm}$ was 1 or less,

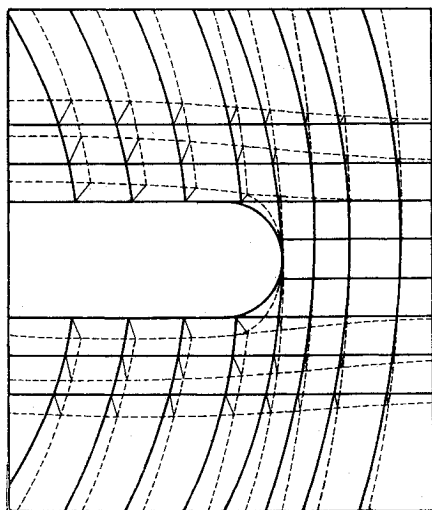


Fig. 17 Distortions produced in grain segment at 25% overall strain at end of star point (solid line shows unstrained grid; dashed line shows distorted grid pattern).

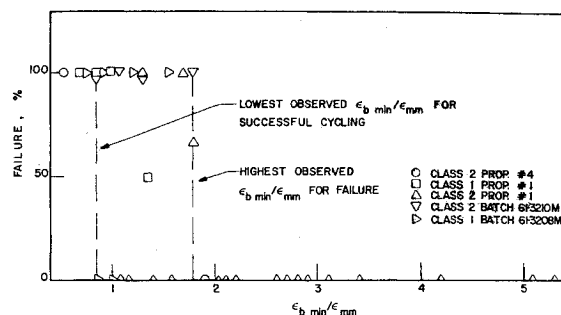


Fig. 18 Summary of failure criteria data.

all of the motors failed; when the ratio was 2 or more, none of the motors failed. The region between 1 and 2 is the expected area of doubt caused by the wide distribution of propellant properties. The relative roles, as described earlier, of the uniaxial and biaxial behaviors of polyurethane propellants should be considered here as a factor in this ratio. As shown in Table 2, the ratio has a mode between 1 and 1.2 for test temperatures down to 0°F . It is felt that this uniaxial-biaxial failure ratio may become a more significant factor at the low temperature of -75°F . Hence, this failure ratio may, in part, account for the large "no-failure" limit of two for the ratio $\epsilon_{b\min}/\epsilon_{mm}$.

Intermediate-Temperature Failure Mode

The intermediate temperature failure mode occurs in large motors held in storage at temperatures below the cure temperature and is related directly to the constant strain failure test. This test has been valuable in providing a basis for correlating motor failure behaviors and laboratory test results. A wide variety of class 2 polyurethane propellants was tested, and the critical constant strain ϵ_c was estimated for each at 40°F . These propellants were employed in experimental motors of both tubular and star configurations varying in grain diameter from 8 in. up to 50 in. The inner bore hoop strain ϵ_{θ} expected on cooling the grain to 40°F was calculated using an elastic analysis, which assumes that the propellant is mechanically incompressible. The percentage of the motors failing due to longitudinal inner bore cracks is plotted in Fig. 19 vs the ratio $\epsilon_c/\epsilon_{\theta}$. For values of the ratio less than 0.8, 100% failures are anticipated, whereas for values of the ratio greater than 1.1 to 1.4, no failures are expected.

The applicability of the failure criteria of Figs. 18 and 19 to full motors is not confirmed yet in a full statistical sense because of the small number of controlled failure studies on large motors. Since failures in full scale motors seldom are produced deliberately because of the cost, the failure analyst must use data taken from unplanned failures where the true strains are not known and the test conditions are confounded by many other variables. Over a long period of time,

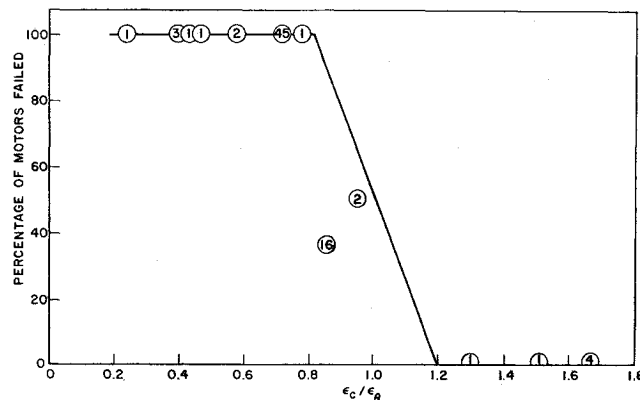


Fig. 19 Motor failures relative to constant strain criteria.

however, data can be accumulated, carefully weighed and evaluated, and compared with the small scale studies. The good agreements already obtained in correlating full-scale motor data amply support the greater use of small-scale studies to develop generalized failure correlations.

Conclusion

The conditions of manufacture, handling, storage, shipment, and use of rocket motors can be reduced to a set of specific critical conditions. Each critical condition can be analyzed and reduced to a combination of stresses or strains and environmental conditions, which, in turn, can be reproduced with some type of laboratory test. Establishing valid failure criteria for propellant grains can be divided into three major parts: first, the prediction and observation of strains and resulting failures in actual motors, second, the laboratory evaluation of failure processes in propellant specimens, and third, the correlation of specimen failure with motor failure.

The analysis of motor stresses and strains has shown good agreement with observed strains and allows a focus on the failure points. For each expected point of failure, the mode and conditions of failure allow selection of corresponding laboratory test conditions. The comparison of simple uniaxial tensile failure with low-temperature motor failure illustrates how a very simple test can prove very useful in a complex failure problem.

The concept of failure necessarily focuses attention on those members of the population most likely to fail. The usual measurement of properties and correlation of data center around mean values, with estimates of variability being made to assess the measurement quality. Stress and strain calculations also focus on the use of mean values of the parameters and comparison of these with mean values of the observed loads and deflections. Failure, however, is concerned with the likelihood of a particular stress or strain occurring at the point where the material properties are least adequate. The formation of yield bands in class 2 and class 3 propellants gives particular point to this problem. The data on these classes suggest that, as the strains increase, yield bands occur and change the distribution of strains, thus producing regions in which failure will occur before further strain is produced in the unyielded regions. Hence, any form of analysis which is based upon an assumption of material homogeneity cannot lead directly to predictions of failure.

The work on failure of propellant specimens has given much insight into the probable mechanism of failure in any highly loaded polymer system. At low temperatures and high rates of strain, failure appears to occur by brittle fracture. At low rates and high temperatures, failure results from a series of processes; first, a breaking of certain binder-

to-oxidizer bonds, followed by tearing in the binder structure initiated at points of stress concentration in the regions of binder-oxidizer dewetting. On the basis of these observations, it is concluded that failure criteria must be developed by procedures that are selected with regard to the temperature and rate of strain conditions at the time and place where failure might occur. Accordingly, brittle fracture theory should be used for high-rate, low-temperature conditions, tear theory for high-temperature, low-rate conditions, and a combination of brittle and tear theories for intermediate conditions.

References

- ¹ Krause, I. and Shaffer, P. W., "Thermal stresses in spherical case-bonded propellant grains," *J. Eng. Ind.*, 144-148 (1962).
- ² Ungar, E. E. and Shaffer, P. W., "Thermally induced bond stresses in case-bonded propellant grains," *ARS J.* 30, 366-368 (1960).
- ³ Williams, M. L., "Some thermal stress design data for rocket grains," *ARS J.* 29, 260-267 (1959).
- ⁴ Daniel, I. M. and Durelli, A. J., "Photothermoelastic analysis of bonded propellant grains," *Exptl. Mech.*, 97-104 (1961).
- ⁵ Sampson, P. C., "A three-dimensional photoelastic method for solution of differential thermal contraction problems in composite structures," Rept. TP-117, Aerojet-General Corp. (1962).
- ⁶ Wiegand, J. H., "Recent advances in mechanical properties evaluation of solid propellants," *ARS J.* 32, 521-527 (1962).
- ⁷ Blatz, P. J., Knauss, W. G., Schapery, L. A., and Williams, W. L., "Fundamental studies relating to systems analysis of solid propellants," *Calif. Inst. Tech., GALCIT 101, Progr. Rept. 6* (June 15, 1960); also Blatz, P. J., Ko, W. L., and Zak, A. P., "Fundamental studies relating to the mechanical behavior of solid propellants, rocket grains and rocket motors," *Calif. Inst. Tech., GALCIT SM 62-27, Progr. Rept. 5* (November 1962).
- ⁸ Bills, K. W., Jr. and Salcedo, F. S., "The swelling of unfilled and highly filled polymers," *J. Appl. Phys.* 32, 2364-2367 (1961).
- ⁹ Bills, K. W., Jr., Swenny, K. H., and Salcedo, F. S., "The tensile properties of highly filled polymers. Effect of filler concentrations," *J. Appl. Polymer Sci.* 4, 259-268 (December 1960).
- ¹⁰ Dietz, A. G. H. and Eirich, F. R. (eds.), *High Speed Testing*, (Interscience Publishers Inc., New York, 1961), Vol. II, pp. 3-12.
- ¹¹ Blatz, P. J. and Ko, W. L., "Application of finite elastic theory to the deformation of rubbery materials," *Trans. Soc. Rheol.* 6, 223-251 (1962).
- ¹² Wiegand, J. H., "Study of mechanical properties of solid propellants," Rept. 0411-10F, Aerojet-General Corp. (1962).
- ¹³ Williams, M. L., Landel, R. F., and Ferry, J. D., "The temperature dependence of relaxation mechanisms in amorphous polymers and other glass-forming liquids," *J. Am. Chem. Soc.* 77, 3701-3707 (1955).
- ¹⁴ Smith, T. L., "Dependence of the ultimate properties of a CR-S rubber on strain rate and temperature," *J. Polymer Sci.* 32, 99-113 (1958).
- ¹⁵ Smith, T. L. and Stedry, P. J., "A time and temperature dependence of the ultimate properties of SBR rubber at constant elongations," *J. Appl. Phys.* 31, 1992-1998 (1960).